Supporting Information

Chemisorption of Water on the Surface of Silicon Microparticles Measured by DNP-Enhanced NMR

Mallory L. Guy, Kipp J. van Schooten, Lihuang Zhu, and Chandrasekhar Ramanathan*

Department of Physics and Astronomy, Dartmouth College, Hanover, New Hampshire 03755, USA

E-mail: chandrasekhar.ramanathan@dartmouth.edu

Material and Methods

Sample Preparation

For the DNP NMR experiments with the dry powder we used a 5 mm^3 cylindrical sample of the Alfa Aesar silicon particles placed in a glass capillary.

The suspended samples were prepared by mixing 100 mg of silicon powder with either 30 μl of 20:80 H_2O:D_2O, 30 μl of 80:20 H_2O:D_2O, and 50 μl of hexane. De-ionized water and a new vial of 99%-enriched D_2O (Cambridge Isotope Labs) were used to prepare the samples. The samples were not de-gassed. A 1 mm^3 volume of the suspension was placed in a glass capillary for the DNP NMR experiments. The experiments on the fresh samples began immediately after sample preparation. After the experiment, the samples remained in the cryostat until they reached room temperature ($\approx$ 12 hours), after which they were stored at ambient temperature for 5 days before being measured again.

FM waveform generation

The 94 GHz FM microwaves are generated using two mixing stages. The modulation is performed in the first mixing stage shown in Figure S1. A triangular frequency-modulated waveform is programmed into a Tektronix AWG 7052 with a given Δf and f_{m}. The carrier frequency for the modulated waveform was chosen to be 500 MHz, much less than the AWG's maximum 5Gs/s sample rate to avoid undersampling.

The 500 MHz frequency modulated signal is first amplified (Minicircuits ZX60-6013E-S+ amplifier), and then mixed with a 3.5 GHz carrier generated with a USB-based microwave synthesizer (Quonset Microwave QM2010-4400) using a T3 Marki Microwave mixer (Marki Microwave T3-06LQP). The output of the mixer is filtered using two Minicircuits filters (VLF-5500+ and VHF-3500+) to eliminate the lower sideband, yielding a triangular modulated signal at 4 GHz. The inset of Figure S1 shows a spectrum analyzer trace of the 500

MHz demodulated signal (blue trace) compared to the Fourier Transform of the file used to program the AWG (red trace). The waveform shown had a modulation bandwidth of 40 MHz and a modulation frequency of 100 kHz. This 4 GHz modulated signal then enters the second mixing stage, where it is mixed with a 90 GHz carrier and filtered to generate a 94 GHz modulated microwave signal which is fed into the DNP probe.[1]

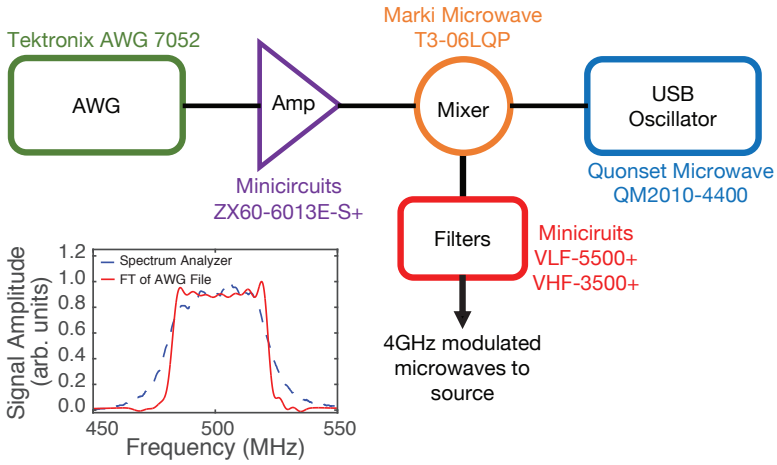

Figure S1: Schematic of the frequency mixing stages used to generate the FM waveform. The plot at the bottom shows a comparison of the fourier transform of the waveform programmed into the AWG, and the frequencies measured on a spectrum analyzer.

SEM and FTIR measurements

The SEM image in Figure 1(b) was taken with a FEI Company XL-30 ESEM-FEG. The silicon particles were mounted to a specimen stage with double-sided tape and loaded into the SEM chamber. The image was acquired with an accelerating voltage of 15 kV and a magnification of 3200x.

The FTIR spectrum in Figure 1(c) was acquired using a JASCO FTIR-6200. A background signal was taken of the chamber without the sample loaded and was used as a background subtraction to the sample spectrum. The sample was then loaded into the chamber after which the chamber was purged with nitrogen gas for 2 minutes. Both spectra were

acquired using 64 scans at 0.5 cm^{-1} resolution. The sample spectrum was baseline corrected by subtracting a 3rd order polynomial fit to the baseline.

Data Analysis

The NMR spectra in all the figures were generated using matNMR.[2] For all the spectra, a DC offset correction was first performed using the average of last 51 points (205-256) of the time-domian FID to estimate the baseline. A left shift of 4 data points was then used to eliminate switching transients and pulse breakthrough effects. Given the 2.5 μs dwell time, this contributed an additional 10 μs to the original 5.5 μs dead time for the detection. Following a 1 kHz exponential line broadening, the data were fourier transformed and phased. To determine the appropriate phasing for the spectra, the highest SNR spectrum in an experimental series was phased and the others were phased identically.

In Figure 1, the thermal spectrum was first attenuated by a factor of 16 to account for differences in experimental receiver gain.

In Figure 2, the best fit was obtained using a single Lorentzian with a linewidth of 6.2 kHz. The enhancements shown in the parameter space image of Figure 2 were obtained using the ratio of amplitudes of the corresponding Lorentzian spectral fits. A high SNR spectrum ($\Delta f = 30$ MHz, $f_{\mathrm{m}} = 10$ kHz) was first fit to characterize the center and width of the spectra. These values were then fixed when fitting the amplitudes of all the other FM DNP spectra, the CF DNP spectrum and the thermal signal. The parameter space explored for the FM DNP contains a total of 50 data points, with the modulation amplitude ranging from 10–100 MHz in increments of 10 MHz and the modulation frequency ranging from 1 kHz to 10 MHz in powers of 10. The LOD-ESR spectra were smoothed using the Matlab smooth function (moving average filter with a span of 100) to reduce the noise level.

In Figure 3, the FM DNP spectra for the H_2O rich sample was fit to a single Lorentzian (the very broad component is unseen because of the left shift of 4 data points). The width

of the Lorentzian was 5.2 kHz, slightly narrower than that observed for the dry powder. The D_2O rich sample and the hexane samples were fit using the sum of a narrow Lorentzian and a broad Gaussian. For the D_2O rich sample, the broad Gaussian had a linewidth of about 13.1 kHz and the narrow Lorentzian had a linewidth of about 5.1 kHz. For the hexane sample, the narrow Lorentzian had a linewidth of about 5.4 kHz and the broad Gaussian had a linewidth of 104 kHz. Once again, a high SNR spectrum (Δf = 30 MHz, f_{m} = 10 kHz) was first fit to characterize the center and width of each of the spectral peaks. These values were then fixed when fitting the amplitudes of the other spectra. The magnitudes of the fits for each component were then used to calculate the reported DNP enhancements. Figure S3 show the two-component fits for the fresh and aged D_2O-rich sample and the hexane sample.

In Figure 4, the amplitudes of the aged spectra were fit using the same center and width parameters determined from the freshly prepared samples. Excellent fits were obtained in all cases. The ratios of the fits to the narrow spectral line were then used to create the maps shown in the figure. Note that we observed small frequency shifts in the spectral peaks in different experiments, and occasionally observed the peaks to shift during a single cool down. We determined that changes in sample placement within the coil, and rotational variations in the probe position could lead to changes of line position by 1 kHz and 600 Hz respectively, due to the inhomogeneity of the magnetic field. The peak shifts during a cool down were due to changes in helium pressure shifting the sample within the coil. In order to compare the spectra from different experimental cooldowns, we shifted the centers of the aged peaks in Figure 4 to ensure overlap. The H_2O-rich spectrum was shifted by 500 Hz, the D_2O-rich spectrum was shifted by 1 kHz, and the hexane spectrum was shifted by 500 Hz.

Supporting Data

Dry baseline signal

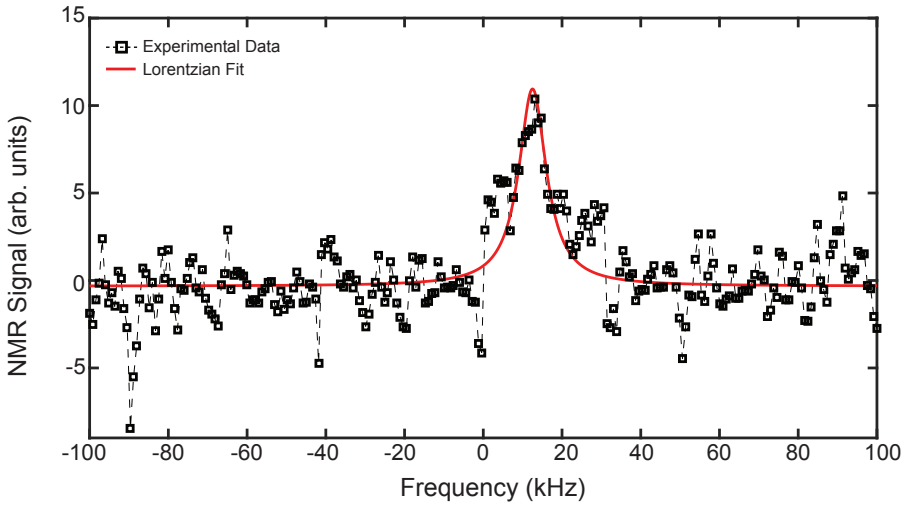

Figure S2: Baseline signal for the dry silicon powder. The data (black squares) is fit to single Lorentzian resonance (red trace) with a linewidth of 6.2 kHz.

Figure S2 shows the single Lorentzian fit to the NMR spectrum of the dry powder in the absence of applied microwaves (no DNP). A high SNR DNP-enhanced proton NMR spectrum (Δf = 30 MHz, f_{m} = 10 kHz) was first fit to characterize the center and width of the spectra (shown in Figure 2 of the main paper). These values were then fixed when determining the best fit to the baseline spectrum – shown in red in the figure. The signal to noise for the baseline spectrum is seen to be about 4, resulting in some uncertainty in the reported DNP enhancements.

Two-component fits

Figure S3 shows the two-component fits for to NMR spectra for the fresh and aged D_2O-rich sample and the hexane sample obtained with FM DNP. The data were fit with two

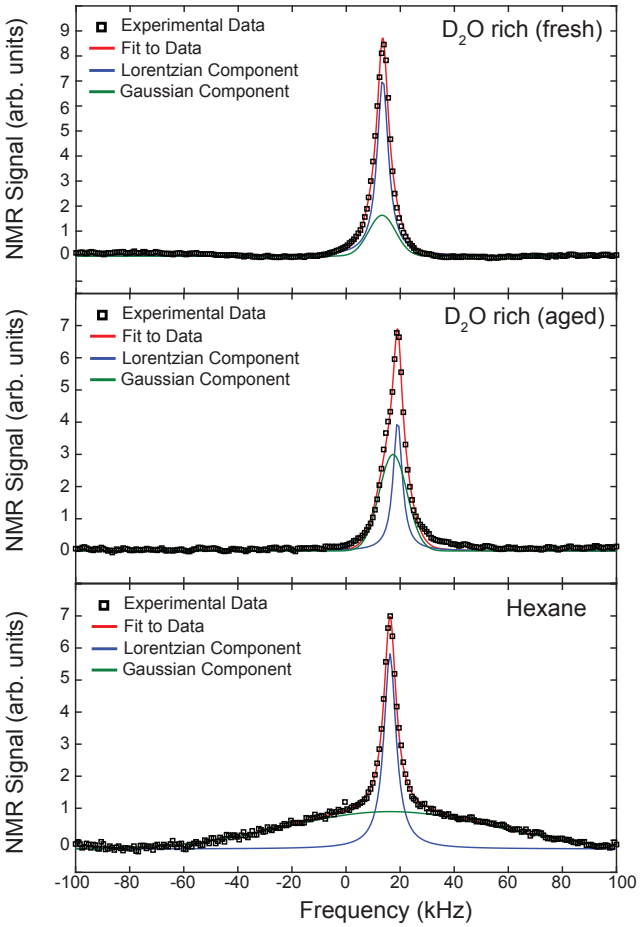

Figure S3: Proton NMR spectra and two-component spectral fits to the broad and narrow resonances for suspended silicon microparticles: (top) D_2O-rich solvent - freshly prepared; (middle) D_2O-rich solvent - aged; (bottom) hexane solvent. The plots show the experimental data (black squares) and total fit (red trace), along with the decomposed broad (green trace) and narrow (blue trace trace) components of the fit. These spectra were obtained using FM DNP with $\Delta f = 30$ MHz and $f_{\mathrm{m}} = 10$ kHz.

components: a narrow Lorentzian line and a broad Gaussian line. For each sample, the linewidth of the narrow component was observed to match that of the dry powder ($\sim$ 5–6 kHz) while the broad component was observed to change with the solvent. For the D_2O-rich sample, the broad component was about 13.1 kHz and the narrow component was about 5.1 kHz for the fresh sample. The width of the narrow component decreased in the aged samples (4.2 kHz), but the width of the broad component was relatively unchanged. For the hexane sample, the linewidth of the broad Gaussian had a linewidth of 104 kHz.

Growth of the DNP signal

We also measured the growth of the DNP signal as a function of millimeter wave irradiation time. Figure S4(a) shows the growth for the dry powder and for the narrow components for the freshly prepared samples of powder dispersed in mixtures of water and D_2O. For each of these, the best fit was obtained with a stretched exponential, similar to those obtained in recent ^{13}C DNP experiments with diamond nanoparticles.[3] For the dry powder, the stretching exponent was 0.80 ± 0.05 and the characteristic time constant was measured to be T= 39 ± 9 s. For the H_2O-rich and D_2O-rich samples the stretching exponents were 0.68 ± 0.04 and 0.66 ± 0.17, respectively, and the characteristic time constants were T= 64 ± 12 s for the H_2O-rich and T= 67 ± 31 s for the D_2O-rich sample, significantly longer than the dry powder. The stretched exponential growth of the narrow component is likely due to a distribution of electron-nuclear interaction strengths, as spin diffusion effects are unlikely to play a role in DNP here. Note that the enhancement observed for the dry particles is higher than that observed for either the H_2O-rich or D_2O-rich samples.

The inset of Figure S4(a) shows the buildup curves for the broad component of the freshly prepared D_2O-rich sample. This was best fit with a sum of two exponentials. The time constants were 339 ± 107 s ($\sim$27 %) and 3528 ± 2034 s ($\sim$73 %) for the D_2O-rich sample. The bi-exponential behavior is due to different compartments of spins at different distances

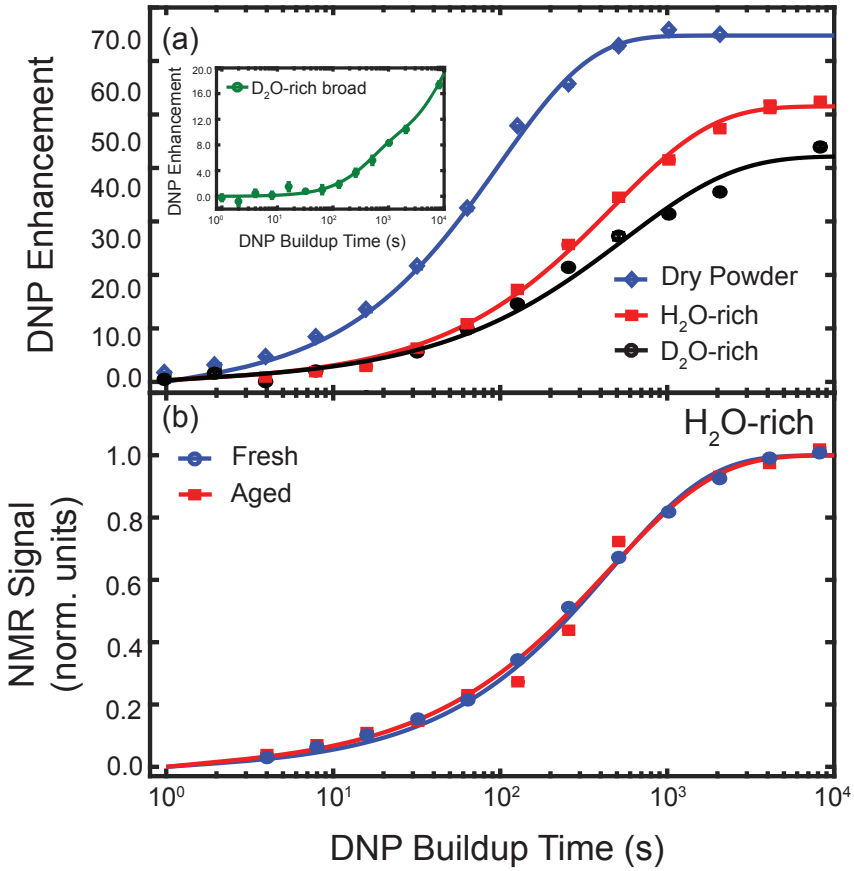

Figure S4: (a) Buildup curves for dry powder (blue diamonds) and narrow components of H_2O-rich (red squares) and D_2O-rich (black circles) samples, and the corresponding stretched exponential fits. The inset shows the growth of the broad component of the D_2O-rich sample, fit with a double exponential. The error bars are smaller than the symbols used. (b) Comparison of the DNP build-up for the fresh (blue circles) and aged H_2O-rich (red squares) sample, showing that the build-up rates are almost unchanged with aging. The error bars are smaller than the symbols used.

to the dangling bond defects. Solvent spins that are closer to the surface of the particles are in direct hyperfine contact with the dangling bond electron spins and experience faster polarization buildup, which those located farther from the particle surface, rely on spin diffusion to polarize.

Figure S4(b) compares the DNP build-up for the fresh and aged H_2O-rich sample, showing that the build-up rates are almost unchanged with sample aging on the 5-day timescale studied. Thus comparisons made at a fixed growth time should accurately reflect the number of spins detected. The stretching exponent for the aged sampled was 0.73 ± 0.09 and the time constant was T= 87 ± 23s. These parameters cannot be statistically distinguished from the parameters for the fresh sample. The error bars for the buildup curves were calculated using the standard deviation of points 160:200 in the time domain (a representative noise-only region for all of the spectra). Since the data points on the curve correspond to spectral fit values from the frequency domain data, a scaling factor of $2N$ (N = buffer size) of the standard deviation of the time domain data was included to accurately represent the calculated error in the frequency domain. The error bars are smaller than the symbols used.

Broad Component Behavior

Figure S5 shows image plots of the ratio of the amplitude of the broad peak in the aged sample to the amplitude of the broad peak in the freshly-prepared sample for all the frequency modulation parameters, for both the D_2O-rich sample (top) and the hexane sample (bottom). The broad component for the D_2O-rich sample sample is seen to increase by about a factor of two during aging, as the surface protons enter solution following exchange with the deuterium. The broad component of the hexane sample remains unchanged, consistent with the narrow component also remaining unchanged. The ratios were calculated using the amplitudes of the fits to the broad spectral components of both the fresh and aged spectra.

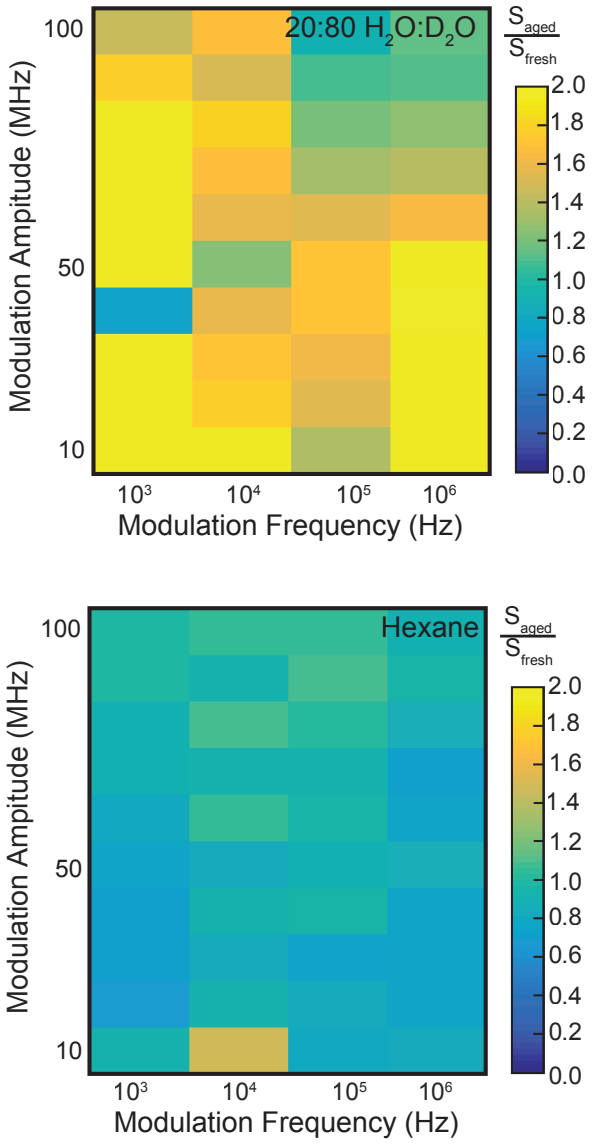

Figure S5: Image plot showing the (top) the change in the broad component for the D_2O-rich sample and (bottom) for the hexane sample. The broad component for the D_2O-rich sample increases by about a factor of 2 while the broad component for the hexane sample remains unchanged.

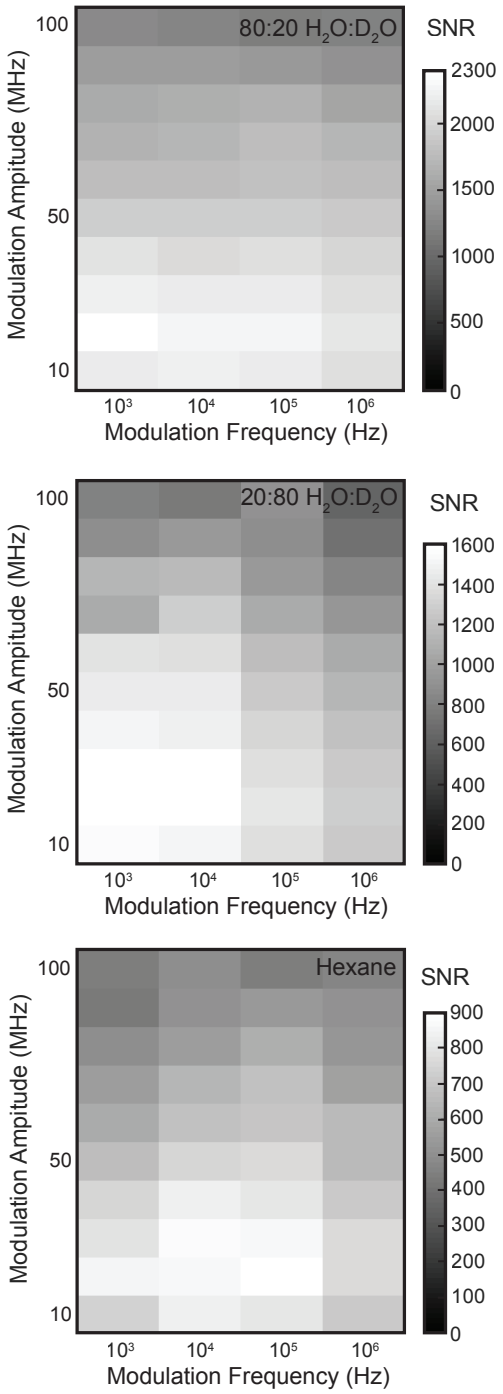

Figure S6: Image plot of the signal-to-noise ratio for proton NMR signal: (top) H_2O-rich sample; (middle) D_2O-rich sample; and (bottom) hexane sample.

Signal-to-Noise Ratios

Figure S6 shows the signal-to-noise ratios for each of the freshly-suspended samples. The standard deviation of the first 10 points in the spectral domain of the baseline signal was used to characterize the noise. This standard deviation was observed to be remain the same across almost all the spectra measured. In some measurements we observed random transient spikes in the time domain - which led to oscillatory features in the baseline, preventing accurate estimates of the noise in individual experiments. The enhancement pattern is similar to that observed with the dry powder (see Figure 2(b) of the main paper).

References

(1) Guy, M. L.; Zhu, L.; Ramanathan, C. Design and characterization of a W-band system for modulated DNP experiments. *J. Magn. Reson.* **2015**, *261*, 11–18.

(2) Van Beek, J. D. matNMR: A flexible toolbox for processing, analyzing and visualizing magnetic resonance data in Matlab®. *J. Magn. Reson.* **2007**, *187*, 19–26.

(3) Rej, E.; Gaebel, T.; Boele, T.; Waddington, D. E. J.; Reilly, D. J. Hyperpolarized nanodiamond with long spin-relaxation times. *Nat. Comm.* **2015**, *6*, 8459.